15-mer DNA Duplexes Containing an Abasic Site Are Thermodynamically More Stable with Adjacent Purines Than with Pyrimidines†

János Sági, Anton B. Guliaev, and B. Singer*

Donner Laboratory, Life Sciences Division, Lawrence Berkeley National Laboratory, University of California, Berkeley, California 94720

Received October 20, 2000; Revised Manuscript Received January 16, 2001

ABSTRACT: Abasic site (AP)-containing duplexes, with flanking adenine (A) or cytosine (C) bases, were shown to be more stable with flanking A than with C bases [Sági, J., Hang, B., and Singer, B. (1999) *Chem. Res. Toxicol. 12*, 917−923]. We investigated whether the lower-magnitude destabilization by an AP site, with A neighbors, is a general effect of the purine versus the pyrimidine neighbors. Duplex stability, as compared to that of the corresponding control duplexes, was markedly decreased by the incorporation of the AP site (x) opposite any of the four bases. However, for the duplexes containing T, A, or C opposite the AP site, replacement of the symmetric doublet flanking pyrimidine bases with purines resulted in a smaller destabilization effect. The average stabilizing effect of the symmetric doublet purine neighbors of an AP site opposite T, A, or C bases was 3.2 °C (ΔT_m) and 1.3 kcal/mol ($\Delta\Delta G°_{37}$) compared to those of pyrimidine neighbors. In contrast, a G·AP pair reduced or eliminated the differential effect of the neighbors. Using unrestrained molecular dynamics, it was shown that for the duplexes containing T opposite the AP site, with doublet pyrimidine neighbors, there was a larger magnitude of curvature around the lesion site than for the duplexes with the purines flanking the AP site. Purines flanking the AP site tend to shift toward each other, creating overlap, in contrast to the flanking pyrimidines. This indicates the possibility of stacking between purine bases at the AP site and can be the reason for the observed smaller thermodynamic destabilization of the duplexes with the AAxAA and GGxGG central sequences, as compared to those with TTxTT and CCxCC sequences. This work showed that for an AP site the GC content is not the only determinant of duplex stability, but rather is influenced more by whether purines or pyrimidines flank the AP site.

Abasic sites in genomic DNA are the most frequent, although rapidly repaired, lesions (*1*, *2*). Stability, conformation, repair, and replication of the abasic sites have been widely studied (*3*−*13*). Recently, we observed a correlation between the thermodynamic stability and the efficiency of cleavage by *Escherichia coli* endonuclease IV of AP[1] site-containing double helices by changing the neighbor sequences adjacent to the AP site (*14*). These neighbor sequences were symmetric triplets in 15-mer duplexes and were composed of A and C nucleotides in different ratios. The AP site, opposite T, strongly destabilized the duplex of each neighbor triplet that was studied. However, when the immediate neighbors of the AP site were C bases, the duplexes were more destabilized than when A bases were flanking the AP site. It could have been expected that the opposite effect could occur with the more stable G·C pair. Since this effect was also observed with triplets with two different GC contents, it was concluded that the effect might be due to more than chance. In the work presented here, this hypothesis is tested with all four possible symmetric doublet neighbors of an AP site, incorporated into 15-mer double helices with all four possible bases opposite the AP site.

Conformational studies of the AP site-containing DNA duplexes showed that the presence of the lesion causes conformational perturbations influenced by the type of opposite (unpaired) base and/or the sequence context. However, the regular B-DNA type geometry was maintained for the whole duplex. Local changes observed at the AP site included the orientation of the opposite base (both extra- and intrahelical positions were observed) (*10*, *15*−*18*), kinking, and the change in groove geometry of the DNA oligomeric duplex (*12*, *17*, *19*, *20*). It has also been shown that the degree of DNA bending is sequence-dependent and is also influenced by the type of opposite base (*21*, *22*). Recently, diffusion rate studies showed that the presence of damaged sites, including AP sites, increased the DNA flexibility (*23*). The increased flexibility close to the AP site was also shown by molecular dynamics simulations (*18*).

The AP site causes significant changes in the thermodynamic stability of a DNA oligonucleotide duplex. Thermodynamics measures the global effect of the lesion on the whole macromolecule and does not show whether structural alterations are global or local. Molecular modeling data showed that these alterations are mainly local, except for the bending. In this work, molecular dynamics simulation

† This work was supported by NIH Grants CA 47723 and CA 72079 (to B.S.) and was administered by the Lawrence Berkeley National Laboratory under Department of Energy Contract DE-AC03-76SF00098.

* To whom correspondence should be addressed. Telephone: (510) 642-0637. Fax: (510) 486-6488. E-mail: singer_lab@lbl.gov.

[1] Abbreviations: AP, apurinic site; MD, molecular dynamics; PME, particle mesh Ewald; ΔT_m, thermal destabilization.

10.1021/bi0024409 CCC: $20.00
Published on Web 03/07/2001

Scheme 1[a]

5' AGCGG NN x NN GAGCT 3'

3' TCGCC NN M NN CTCGA 5'

[a] Where x is an AP site or A, T, C, or G, M is T, A, G, or C, and N is T, A, G, or C.

was used for studies of groups of structures to find a conformational answer to the general observations obtained by thermodynamics, that is, for the differential effect of neighbor bases of an AP site on destabilization. For this purpose, 15-mer duplex structures containing T opposite an AP site (x) were used with four sequence contexts: TTxTT, AAxAA, GGxGG, and CCxCC. The use of the explicit solvent, counterions, and particle mesh Ewald method for the treatment of the electrostatic interactions in the modeling procedure should provide a realistic representation for the highly charged DNA system. Using the same molecular modeling approach, this laboratory showed that the conformational changes induced by the presence of an 1,N^6-ethenoadenine adduct with various sequence contexts correlated with the thermodynamic stability of these 15-mer duplexes (*24*).

MATERIALS AND METHODS

Oligonucleotides. The 15-nucleotide unmodified control, as well as the abasic site (AP)-containing oligodeoxyribonucleotides were purchased from Operon Technologies, Inc. (Alameda, CA) in HPLC-purified form. The "AP" oligonucleotides contained a stabilized form of the AP site, the tetrahydrofuranyl residue which can be incorporated by standard phosphoramidite chemistry using the phosphoramidite of 1′,2′-deoxyribose (dSpacer, from Glen Research, Sterling, VA). The sequences used are given in Scheme 1.

Determination of the Thermodynamic Stability. The nonself-complementary double helices were composed on a 1:1 molar basis. The molar absorbance for the single strands was calculated by the nearest neighbor approximation using the DNA/Oligo Quantitation software of a Beckman DU 7400 spectrophotometer, as described previously (*14*). Double helices with a total strand concentration (C_t) of 8 μM were dissolved in 0.1 M NaCl, 10 mM sodium phosphate buffer, and 0.25 mM Na_2EDTA (pH 7.0). The absorption−melting temperature profiles were recorded in a Beckman DU 7400 diode array spectrophotometer from 5 to 105 °C at 280 nm, essentially as described previously (*14*, *25*). The thermal stability (T_m) and thermodynamic parameters for duplex strand dissociation ($\Delta H°$, $\Delta S°$, and $\Delta G°_{37}$) were calculated from the melting curves of the duplexes, using the MeltWin version 3.0 program (*26*).

Molecular Dynamic Simulations. The apurinic base was constructed by replacing the base of the adenine residue (A) with the hydrogen H1″, using the xLeap module of AMBER 5.0 (*27*). To obtain molecular mechanics parameters for the apurinic base site, ab initio quantum mechanics calculations were employed using the HyperChem 4.5 program (Hypercube, Inc.). Atom-centered charges were obtained by fitting the electrostatic potential calculated ab initio at the 6-311G** basis set level from coordinates optimized at the 3-21G level using the routines provided by the HyperChem program. AMBER atom types were assigned according to published guidelines, and torsional and bond stretching constants were scaled according to bond length (*28*). AMBER topology and parameter files for the four B-DNA duplexes containing 5′-AGCGGGGxGGGAGCT-3′, 5′-AGCGGCCxCCGAGCT-3′, 5′-AGCGGAAxAAGAGCT-3′, or 5′-AGCGGTTxTTGAGCT-3′, where x is an AP site, and the corresponding complementary strands were generated using xLeap. Additionally, four DNA duplexes of the same sequence with the AP site replaced with normal A were used as controls in the simulations. The molecular modeling procedure described below has been utilized for all eight DNA duplexes and described in detail in a previous publication from this laboratory (*24*).

To neutralize negative charges on phosphates, 28 Na^+ ions were placed around phosphate groups. A rectangular box was added providing at least 10 Å of explicit TIP3P water molecules around each DNA duplex. At first, the water box was subjected to a series of equilibration molecular dynamics (MD) runs, while holding the solute fixed. Subsequent equilibration steps, during which position constraints on solute molecules were gradually relaxed, as well as the final production runs, were carried out by using the particle mesh Ewald (PME) method to treat electrostatic interaction. Finally, series of energy minimization runs were performed, during which positional restraints were reduced by 5.0 kcal/mol each round. The unrestrained MD production runs of 500 ps were initiated after heating the system from 10 to 300 K over the course of 10 ps. This simulation length has been used successfully to obtain structural parameters for the other adduct-containing DNA duplexes (*24*, *29*).

The MD trajectories were analyzed using the CARNAL module of AMBER 5.0. The final structure for each duplex was produced by 1000 steps of minimization of the averaged structure from the last 250 ps of MD and analyzed with CURVES 5.3 to calculate the DNA curvature and base pair parameters (*30*). The terminal base pairs were omitted in our analysis due to the known fraying effects, which were also observed in the simulations. Molecular structures were displayed and visually analyzed using Insight II (Insight II 98.0, Biosym/MSI, San Diego, CA). All calculations were performed on a Silicon Graphics Origin 200 server interfaced with an O2 workstation (Silicon Graphics, Inc., Mountain View, CA).

RESULTS

Thermodynamics

Melting of 15-nucleotide unmodified (control) duplexes, as measured previously in this and other laboratories (*14*, *25*, *31*, *32*), showed a clear "two-state" process, where only duplex and single-stranded coil molecular species are supposed to be present at any temperature that was studied. Thermal dissociation of the AP site-containing 15-mers was also shown (*14*) to fit into the concept of two-state melting (*33*, *34*), even if sequence influenced exact molecularity in some cases (*6*). The two-state nature of melting made possible the use of the MeltWin software designed to extract thermodynamic parameters from equilibrium melting curves (*26*). The melting curve of each duplex that was studied was cooperative and reversible, and could be analyzed with MeltWin in the ±30 °C range of T_m values with good curve fitting (X^2 values were in the range of 10^{-7}). The melting curve with the corresponding fit generated by MeltWin is

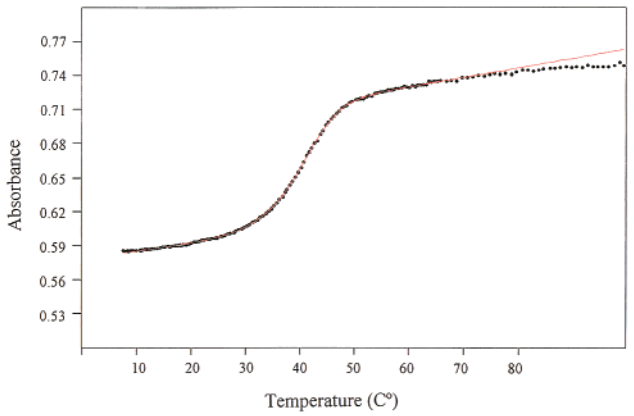

FIGURE 1: Melting curve (·) and corresponding fit (red line) generated by MeltWin for the AP-containing 15-mer oligomer with the central sequence AAxAA (x is AP). See Table 2 for the thermodynamic parameters.

shown in Figure 1. Tables 1−5 contain the thermodynamic parameters for melting, calculated by MeltWin ($\Delta H°$, $\Delta S°$, $\Delta G°_{37}$, and T_m at a duplex concentration of 8 μM), the differential values for stability (ΔT_m and $\Delta\Delta G°_{37}$), and the thermally induced increase in absorbance from 10 to 100 °C at 280 nm (H_{280}). The latter value was calculated directly from the melting curve recorded with the Beckman spectrophotometer.

Control Duplexes

Data for the thermodynamics of dissociation of the unmodified, control duplexes are shown in Table 1. The T_m values for these 15-mer duplexes ranged from 56 to 76 °C in buffered 0.1 M NaCl. It changed according to the GC content when the doublet neighbors were changed from TT, AA, CC, or GG to an A·T, T·A, C·G, or G·C pair, respectively, in the middle of the duplex. The thermal stability of the duplexes with the same GC content also changed with sequence, that is, when the doublet base pairs were flipped. The changes ranged from 0.8 to 6.3 °C. The large effects were observed with GC doublets, such as between duplexes 3 and 4, and 11 and 12. The thermal hyperchromicity (H_{280}) also increased with GC content. However, sequence also had an effect. This effect was more pronounced with the same duplexes that showed a large difference in the T_m values on alteration of sequence (duplexes 5 and 6, and 11 and 12).

The free energy change values for strand dissociation ($\Delta G°_{37}$) generally followed the T_m values with the exception of a few duplexes with high GC content. This was duplex 11 where $\Delta G°_{37}$ was lower than expected from the high T_m value. Enthalpy and entropy values were also lower. Thermodynamic values for duplex 12, which contains eight G·C pairs in a row, were, however, in line with those of the other duplexes. A further example of a lower-than-expected $\Delta G°_{37}$ value is that of duplex 16.

Effect of the Sequence of Doublet Neighbors of an AP Site on the Destabilization of 15-mer Duplexes as a Function of the Opposite Base

Thymine Opposite the AP Site. In the initial experiments, the central AP site flanked by symmetric doublet nucleotides in the 15-mer double helices was incorporated opposite a thymine (Scheme 1). Thermodynamic parameters characterizing the thermally induced dissociation of the duplexes are shown in Table 2.

The presence of the stabilized, tetrahydrofuranyl AP site strongly destabilized all four duplexes, from about 14 to 20 °C and 5.6 to 7.4 kcal/mol. The changes in thermal stability followed the changes in GC content, modulated by sequence (Table 2, duplexes 17−20). Hyperchromicity changes (H_{280}) were also a function of GC content. Free energy change values ($\Delta G°_{37}$) followed the thermal stability values. The

Table 1: Thermodynamic Parameters for the Thermal Dissociation of 15-mer Control Duplexes As Determined by MeltWin Analysis of the Beckman Melting Curves[a]

		MeltWin analysis of the Beckman melting curves				
#	Central sequence	T_m (°C)	H_{280} (%)	$\Delta H°$ (kcal/mol)	$\Delta S°$ (cal/K mol)	$\Delta G°_{37}$ (kcal/mol)
1	-TTATT- -AATAA-	58.4 ± 0.2	31.4	108.1 ± 1.0	300.0 ± 3.2	15.07 ± 0.02
2	-AAAAA- -TTTTT-	57.6 ± 0.2	32.6	107.9 ± 2.2	300.2 ± 6.9	14.59 ± 0.32
3	-CCACC- -GGTGG-	71.7 ± 0.4	49.1	120.5 ± 0.4	323.4 ± 1.5	20.20 ± 0.07
4	-GGAGG- -CCTCC-	66.1 ± 0.2	40.9	117.9 ± 0.4	321.3 ± 0.7	18.21 ± 0.11
5	-TTTTT- -AAAAA-	60.3 ± 0.2	36.4	107.3 ± 0.1	295.8 ± 0.1	15.59 ± 0.05
6	-AATAA- -TTATT-	57.0 ± 0.1	32.9	106.3 ± 0.9	296.0 ± 2.7	14.52 ± 0.05
7	-CCTCC- -GGAGG-	71.0 ± 0.1	46.1	113.7 ± 2.0	304.2 ± 6.0	19.32 ± 0.23
8	-GGTGG- -CCACC-	68.3 ± 0.3	46.6	111.1 ± 1.1	299.2 ± 3.0	18.27 ± 0.18
9	-TTGTT- -AACAA-	63.0 ± 0.2	38.6	112.5 ± 1.1	308.5 ± 2.9	16.79 ± 0.14
10	-AAGAA- -TTCTT-	59.5 ± 0.1	36.2	108.8 ± 1.0	301.1 ± 3.0	15.46 ± 0.07
11	-CCGCC- -GGCGG-	75.6 ± 0.2	54.6	98.2 ± 1.5	255.5 ± 4.6	18.94 ± 0.14
12	-GGGGG- -CCCCC-	69.3 ± 0.1	34.9	118.4 ± 2.1	319.6 ± 6.3	19.23 ± 0.17
13	-TTCTT- -AAGAA-	61.8 ± 0.4	32.8	104.4 ± 0.4	285.6 ± 0.9	15.80 ± 0.12
14	-AACAA- -TTGTT-	60.5 ± 0.2	33.0	111.4 ± 2.5	307.6 ± 7.8	15.95 ± 0.14
15	-CCCCC- -GGGGG-	72.3 ± 0.3	44.8	104.0 ± 1.1	275.1 ± 3.5	18.70 ± 0.03
16	-GGCGG- -CCGCC-	70.5 ± 0.1	46.8	101.2 ± 0.9	268.3 ± 2.8	17.94 ± 0.11

[a] The absorption (280 nm) vs temperature melting curves were measured with duplex concentrations of 8 μM in 0.1 M NaCl, 0.01 M sodium phosphate, and 0.25 mM Na_2EDTA, with the pH adjusted to 7.0; H_{280} refers to the increase in absorption at 280 nm from 10 to 100 °C. The standard error for H_{280} was ±1.3%.

Table 2: Effect of the Change of Doublet Neighbors at an AP Site Opposite T on the Destabilization of 15-mer Duplexes As Determined by MeltWin Analysis of the Beckman Melting Curves[a]

		MeltWin analysis of the Beckman melting curves						
#	Central sequence	T_m (°C)	ΔT_m (°C)	H_{280} (%)	ΔH^o (kcal/mol)	ΔS^o (cal/K mol)	ΔG^o_{37} (kcal/mol)	$\Delta\Delta G^o_{37}$ (kcal/mol)
17 (c1)	-TTxTT- -AATAA-	39.0 ± 0.1	-19.4 ± 0.2	32.6	61.4 ± 0.1	170.6 ± 0.2	8.50 ± 0.02	-6.57 ± 0.03
18 (c2)	-AAxAA- -TTTTT-	40.3 ± 0.1	-17.3 ± 0.2	29.4	81.2 ± 1.0	233.0 ± 3.1	8.94 ± 0.02	-5.65 ± 0.34
19 (c3)	-CCxCC- -GGTGG-	55.9 ± 0.3	-15.8 ± 0.1	45.9	82.3 ± 0.5	224.0 ± 1.8	12.81 ± 0.04	-7.39 ± 0.03
20 (c4)	-GGxGG- -CCTCC-	52.2 ± 0.4	-13.9 ± 0.1	45.0	94.1 ± 0.4	263.2 ± 1.2	12.47 ± 0.12	-5.74 ± 0.01

[a] The absorption (280 nm) vs temperature melting curves were measured with duplex concentrations of 8 μM in 0.1 M NaCl, 0.01 M sodium phosphate, and 0.25 mM Na_2EDTA, with the pH adjusted to 7.0; H_{280} refers to the increase in absorption at 280 nm from 10 to 100 °C. The standard error for H_{280} was ±1.3%. The letter c and the number in parentheses refer to the corresponding number of the control duplexes in Table 1.

ΔT_m values were larger with the TT or AA duplexes (Table 2, duplexes 17 and 18) than with the CC or GG duplexes (duplexes 19 and 20). That is, the duplexes with higher GC content at the AP site were apparently less destabilized, as determined by the ΔT_m values, than the duplexes with lower GC content. However, $\Delta\Delta G°_{37}$ values did not follow the ΔT_m values. Instead, these values could be correlated with the sequence at the AP site. When this sequence contained purines, the $\Delta\Delta G°_{37}$ values were smaller than those of the sequences that contained pyrimidines.

The thermal stability (T_m) of the two AP duplexes with AA or TT neighbors was similar (Table 2, duplexes 17 and 18) and varied with sequence to only a small extent. Destabilizations, as compared to the controls (Table 1, duplexes 1 and 2), differed by about 2 °C in the ΔT_m and 1 kcal/mol in the $\Delta\Delta G°_{37}$ values. The stability of the two duplexes with CC or GG neighbors (Table 2, duplexes 19 and 20) varied significantly with sequence, as did the controls (Table 1, duplexes 3 and 4). However, destabilizations also differed by about 2 °C and 1.6 kcal/mol. The purine neighbors allowed less destabilization of the duplex by the AP site than the pyrimidine neighbors.

Transition enthalpy ($\Delta H°$) and entropy ($\Delta S°$) values generally change with the GC content of the unmodified duplex, modulated by sequence. However, in the case of this group of AP site-containing duplexes (Table 2, duplexes 17−20), enthalpy and entropy values were different for the duplexes with the same GC content, although $\Delta G°_{37}$ values were similar (duplexes 17 and 18, and 19 and 20). The enthalpy value was smaller when pyrimidine bases flanked the AP site, compared to when purine bases were the immediate neighbors.

Adenine Opposite the AP Site. Adenine, cytosine, and guanine were also incorporated opposite the AP site (Tables 3−5) to test the stabilization effect of purine neighbors, as compared to pyrimidines, observed for the duplexes with T opposite the AP site (Table 2). The stability of duplexes with adenine opposite the AP site (Table 3, duplexes 21−24) showed an effect similar to that observed with duplexes containing T opposite the AP site. The AP site destabilized the 15-mer duplexes more when the symmetric flanking doublets of the AP site were TT nucleotides (duplex 21) as compared to AA nucleotides (duplex 22), or the CC nucleotides (duplex 23) as compared to the GG duplex (duplex 24). The average difference was about 1.5 °C in the ΔT_m values and 1.15 kcal/mol in the $\Delta\Delta G°_{37}$ values.

The T_m and also the $\Delta G°_{37}$ values were higher in this group of duplexes than in those with thymine opposite the AP site (Table 2, duplexes 17−20), although the GC contents were the same. The ΔT_m values were, however, lower than those of the corresponding duplexes in Table 2, although the tendency was the same; the higher GC content allowed less destabilization (duplexes 23 and 24), and purine neighbors (duplexes 22 and 24) allowed less destabilization than did the pyrimidine neighbors (duplexes 21 and 23). The $\Delta H°$ values were higher for the duplexes with purine neighbors than for the corresponding duplexes with flanking pyrimidines (duplexes 22 vs 21 and 24 vs 23), and there also was a minimum difference of 1 kcal/mol in the $\Delta\Delta G°_{37}$ values, similar to the results for the group of duplexes with T opposite the AP site.

Cytosine Opposite the AP Site. Table 4 contains the thermodynamic data for the duplexes which contained a C base opposite the AP site (duplexes 25−28). The T_m and also the $\Delta G°_{37}$ values were lower for this group of duplexes than for the corresponding duplexes with T or A opposite the AP site (Tables 2 and 3), although the GC contents were higher. On the other hand, the ΔT_m values were much higher in this group than in the groups of duplexes with T or A opposite bases. The higher GC content (Table 4, duplexes 27 and 28) resulted in an average duplex destabilization lower than the AT content (duplexes 25 and 26), although there was some overlapping (duplex 27). The difference in the ΔT_m value between duplexes with doublet purine flankings versus the duplexes with doublet pyrimidine flankings (duplexes 25 vs 26 and 27 vs 28) was greater than 2 °C, observed for the other two groups (Tables 2 and 3). The AP duplex with AA neighbors (duplex 26) was less destabilized

Table 3: Effect of the Change of Doublet Neighbors at an AP Site Opposite A on the Destabilization of 15 Duplexes As Determined by MeltWin Analysis of the Beckman Melting Curves[a]

		MeltWin analysis of the Beckman melting curves						
#	Central sequence	T_m (°C)	ΔT_m (°C)	H_{280} (%)	ΔH^o (kcal/mol)	ΔS^o (cal/K mol)	ΔG^o_{37} (kcal/mol)	$\Delta\Delta G^o_{37}$ (kcal/mol)
21 (c5)	-TT**x**TT- -AA**A**AA-	42.5 ± 0.1	-17.8 ± 0.1	33.0	68.2 ± 1.2	189.8 ± 4.0	9.28 ± 0.02	-6.31 ± 0.03
22 (c6)	-AA**x**AA- -TT**A**TT-	41.5 ± 0.1	-15.5 ± 0.1	29.8	85.0 ± 0.8	244.0 ± 2.6	9.30 ± 0.05	-5.22 ± 0.04
23 (c7)	-CC**x**CC- -GG**A**GG-	58.1 ± 0.1	-12.9 ± 0.1	47.4	87.4 ± 0.5	237.6 ± 1.5	13.65 ± 0.05	-5.67 ± 0.18
24 (c8)	-GG**x**GG- -CC**A**CC-	56.0 ± 0.1	-12.3 ± 0.3	44.7	98.6 ± 2.8	273.4 ± 8.4	13.79 ± 0.16	-4.48 ± 0.02

[a] The absorption (280 nm) vs temperature melting curves were measured with duplex concentrations of 8 μM in 0.1 M NaCl, 0.01 M sodium phosphate, and 0.25 mM Na_2EDTA, with the pH adjusted to 7.0; H_{280} refers to the increase in absorption at 280 nm from 10 to 100 °C. The standard error for H_{280} was ±1.3%. The letter c and the number in parentheses refer to the corresponding number of the control duplexes in Table 1.

Table 4: Effect of the Change of Doublet Neighbors at an AP Site Opposite C on the Destabilization of 15 Duplexes As Determined by MeltWin Analysis of the Beckman Melting Curves[a]

		MeltWin analysis of the Beckman melting curves						
#	Central sequence	T_m (°C)	ΔT_m (°C)	H_{280} (%)	ΔH^o (kcal/mol)	ΔS^o (cal/K mol)	ΔG^o_{37} (kcal/mol)	$\Delta\Delta G^o_{37}$ (kcal/mol)
25 (c9)	-TT**x**TT- -AA**C**AA-	38.3 ± 0.1	-24.7 ± 0.2	30.0	62.8 ± 0.4	175.3 ± 1.6	8.35 ± 0.02	-8.44 ± 0.12
26 (c10)	-AA**x**AA- -TT**C**TT-	39.1 ± 0.1	-20.4 ± 0.1	29.8	80.9 ± 0.6	232.9 ± 1.9	8.62 ± 0.02	-6.84 ± 0.08
27 (c11)	-CC**x**CC- -GG**C**GG-	53.1 ± 0.1	-22.5 ± 0.3	44.8	65.4 ± 1.2	174.2 ± 3.9	11.32 ± 0.06	-7.62 ± 0.19
28 (c12)	-GG**x**GG- -CC**C**CC-	55.1 ± 0.1	-14.2 ± 0.2	44.7	90.2 ± 1.6	248.8 ± 4.9	13.04 ± 0.12	-6.19 ± 0.04

[a] The absorption (280 nm) vs temperature melting curves were measured with duplex concentrations of 8 μM in 0.1 M NaCl, 0.01 M sodium phosphate, and 0.25 mM Na_2EDTA, with the pH adjusted to 7.0; H_{280} refers to the increase in absorption at 280 nm from 10 to 100 °C. The standard error for H_{280} was ±1.3%. The letter c and the number in parentheses refer to the corresponding number of the control duplexes in Table 1.

by 4.3 °C and 1.6 kcal/mol than the duplex with TT neighbors (duplex 25). Similarly, the AP duplex with GG neighbors was less destabilized by 8.3 °C and 1.43 kcal/mol than the AP duplex with CC neighbors (duplexes 27 and 28). The enthalpy values were higher for the duplexes with purine neighbors, as compared to those for duplexes with pyrimidine flankings, and the enthalpy was well compensated by entropy in all cases which resulted in similar $\Delta G°_{37}$ values for duplexes with the same GC content. Effective enthalpy−entropy compensation was also observed with AP duplexes containing T or A opposite (Tables 2 and 3). The $\Delta\Delta G°_{37}$ values were large, and the duplexes with purine flanking doublets (duplexes 26 and 28) were less destabilized than the duplexes with pyrimidine flanking doublets (duplexes 25 and 27) by more than 1 kcal/mol.

The average difference in duplex destabilization by an AP site opposite a T, A, or C base was 3.2 °C for the ΔT_m values and 1.3 kcal/mol for the $\Delta\Delta G°_{37}$ values when the AP site was flanked by AA or GG bases instead of by TT or CC bases (Tables 2−4).

Guanine Opposite the AP Site. Destabilization of the AP duplexes was different when G was the opposite base (Table 5, duplexes 29−32) compared to T, A, or C as the opposite base. With G opposite the AP site, there was a 1.5 °C difference in the ΔT_m values between duplexes with TT or AA neighbors (duplexes 29 and 30); however, a difference of only 0.12 kcal/mol was found between the $\Delta\Delta G°_{37}$ values. With the duplexes containing CC or GG neighbors, an opposite effect was observed; the duplex with the GG neighbor was more destabilized, by 0.24 kcal/mol and −2.4 °C in the ΔT_m , than the duplex with the CC neighbor (duplexes 31 and 32). On average, the opposite G abolished or changed the differential effect of the neighbors of the AP site on destabilization, as compared to the effects observed

Table 5: Effect of the Change of Doublet Neighbors at an AP Site Opposite G on the Destabilization of 15 Duplexes As Determined by MeltWin Analysis of the Beckman Melting Curves[a]

		MeltWin analysis of the Beckman melting curves						
#	Central sequence	T_m (°C)	ΔT_m (°C)	H_{280} (%)	ΔH^o (kcal/mol)	ΔS^o (cal/K mol)	ΔG^o_{37} (kcal/mol)	$\Delta\Delta G^o_{37}$ (kcal/mol)
29 (c13)	-TTxTT- -AAGAA-	41.9 ± 0.2	-19.9 ± 0.1	33.0	70.9 ± 0.3	199.0 ± 1.0	9.18 ± 0.04	-6.62 ± 0.08
30 (c14)	-AAxAA- -TTGTT-	42.1 ± 0.1	-18.4 ± 0.1	31.2	84.4 ± 2.1	241.7 ± 6.8	9.45 ± 0.01	-6.50 ± 0.12
31 (c15)	-CCxCC- -GGGGG-	60.0 ± 0.3	-12.3 ± 0.1	43.5	92.7 ± 2.1	252.0 ± 6.4	14.49 ± 0.21	-4.21 ± 0.24
32 (c16)	-GGxGG- -CCGCC-	55.8 ± 0.1	-14.7 ± 0.2	41.8	94.7 ± 1.5	261.9 ± 4.6	13.49 ± 0.08	-4.45 ± 0.19

[a] The absorption (280 nm) vs temperature melting curves were measured with duplex concentrations of 8 μM in 0.1 M NaCl, 0.01 M sodium phosphate, and 0.25 mM Na_2EDTA, with the pH adjusted to 7.0; H_{280} refers to the increase in absorption at 280 nm from 10 to 100 °C. The standard error for H_{280} was ±1.3%. The letter c and the number in parentheses refer to the corresponding number of the control duplexes in Table 1.

with T, A, or C opposite (Tables 2−4).

The effect of GC content on thermal destabilization (ΔT_m) was, however, the same as that observed with the other three groups of duplexes that were studied; the higher GC content (duplexes 31 and 32) showed less thermal destabilization by the AP site than did the higher AT content (duplexes 29 and 30). The enthalpy values were different for only the duplexes with A·T base pair neighbors (duplexes 29 and 30) and not for those observed for the other groups in Tables 2−4. However, for duplexes 31 and 32, enthalpy values were very similar.

Molecular Dynamics Simulations

Overall Structure. The overall stability of the simulations was evaluated by calculating root mean square deviation (rmsd) values of each 1 ps "snapshot" relative to the coordinates of the initial (energy-minimized) structures for all four lesion-containing duplexes and the corresponding controls. The duplex structures containing TTxTT and CCxCC central sequences reached the conformational equilibrium, and rmsd values plateaued after 150 ps. The equilibrium for the AAxAA and GGxGG structures was observed after 200 and 250 ps, respectively. Therefore, only conformations generated during the 250−500 ps period of simulations were used to monitor the structural properties. Higher average rmsd values were measured for the TTxTT and AAxAA structures (3.66 ± 0.8 and 3.2 ± 0.8 Å, respectively) than for the CCxCC and GGxGG structures (2.31 ± 0.5 and 2.44 ± 0.5 Å, respectively). All four AP site-containing structures remained in the B-DNA conformational family during the entire simulation. Previously reported NMR studies supported the B-conformation for the AP-containing DNA duplexes (*12*, *17*, *20*, *35*). The base pairs immediately adjacent to the AP site showed some perturbation in the inter- and intra-base pair parameters. An extrahelical conformation for the unpaired T was not observed. However, significant perturbation in the interbase parameters for the unpaired T and the preceding base step was observed for the structures with the pyrimidines flanking the AP site (TTxTT and CCxCC) (Table 6). These perturbations were primarily observed for inter-base pair parameters such as roll, twist, and tilt. In the case of the TTxTT structure, the roll value for the A24/T23 base step was about 2 times higher than for the control structure, TTATT (Table 6). A larger roll was also observed for the CCxCC structure. In the case of purines flanking the AP site, the roll values for the T24/T23 step with the AAxAA structure and for the C24/T23 step with the GGxGG structure remained close to the values observed for the controls. The twist values for the same base steps indicated untwisting of DNA at the AP site for the structures with the pyrimidines flanking the AP site. A value of 13° was observed for the A24/T23 step in the TTxTT structure and 14° for the G24/T23 step in the CCxCC duplex. It should be noted that the small values for the twist parameter of the AAAAA control structure can account for the known high flexibility of the A tracts in DNA (*36*).

Table 6: Global Interbase Parameters for the T Opposite the AP Site

Base step*	Tilt (°)		Roll (°)		Twist (°)	
	X=A	X=AP	X=A	X=AP	X=A	X=AP
A24/T23 -T_6 T_7 $\mathbf{x_8}$ T_9 T_{10}- -$A_{25}A_{24}\mathbf{T_{23}}A_{22}A_{21}$-	3	-9	-16	-35	31	13
T24/T23 -A_6 A_7 $\mathbf{x_8}$ A_9 A_{10}- -T_{25} T_{24} $\mathbf{T_{23}}$ T_{22} T_{21}-	-7	-8	-14	-14	21	21
G24/T23 -C_6 C_7 $\mathbf{x_8}$ C_9 C_{10}- -$G_{25}G_{24}\mathbf{T_{23}}$ $G_{22}G_{21}$-	6	-19	11	-27	34	14
C24/T23 -G_6 G_7 $\mathbf{x_8}$ G_9 G_{10}- -$C_{25}C_{24}$ $\mathbf{T_{23}}$ $C_{22}C_{21}$-	-3	-14	-13	-19	34	51

[a] In each case, the base step that was analyzed consisted of thymine opposite the AP site and the preceding base. The values have been rounded up to the nearest whole number.

Curvature as a Function of Flanking Bases. The magnitude of DNA bending was also calculated for all four AP-containing and four control duplexes. The values for bending as a function of the number of base pairs can be found in Table 7. From these data, it can be seen that the magnitude of bending depends largely on the length of the analyzed

Table 7: Bending vs Central Oligonucleotide Length

Central Sequence	Bending (°)*							
	15bp		11bp		7bp		5bp	
	X=A	X=AP	X=A	X=AP	X=A	X=AP	X=A	X=AP
-TT **x** TT- -AA**T**AA-	14	5	8	22	4	30	6	18
-AA **x** AA- -TT **T** TT-	15	18	13	16	10	11	4	9
-CC**x**CC- -GG**T**GG-	10	19	8	19	6	16	7	12
-GG**x**GG- -CC**T**CC-	7	17	4	12	9	13	8	11

[a] The values have been rounded up to the nearest whole number.

segment. In the following analysis, only values for the truncated 11-mer duplexes (central 11 base pairs) will be discussed to avoid the contribution of the terminal bases, which showed fraying effects during the simulation. In all four AP duplexes, the presence of the AP site increased the magnitude of the DNA curvature in comparison with the values observed for the controls (Table 7). For the structure containing the AAAAA central sequence, or A tract, there was only a small increase in the curvature when the central A was replaced with the AP site (13° vs 16°, respectively). However, in the structures with the pyrimidines flanking the AP site (TTxTT and CCxCC) curvature values were larger than for the structures with the purine bases flanking the AP site (AAxAA and GGxGG).

Base Overlapping as a Function of the Flanking Sequence at the AP Site. The top views of the central 3 bp motif of all eight averaged minimized structures produced by the modeling are shown in Figure 2. In all four control structures, the bases flanking the central A showed almost no overlapping (Figure 2, right panel). In the case of the AP duplexes with TTxTT and CCxCC central sequences (Figure 2, left panel, top two structures), some displacement of the bases flanking the AP site toward each other can be seen, but no significant overlap was observed, as compared to the controls. However, in the AP site-containing duplexes with AAxAA and GGxGG central sequences (Figure 2, left panel, the two bottom structures), a significant overlapping can be seen between the two bases flanking the AP site. This may be an indication of a distant, weak stacking interaction, which was produced by the molecular dynamics simulation. Note that the starting structures for the AAxAA and GGxGG duplexes were generated as B-DNA and have no overlap between the bases flanking the AP site.

DISCUSSION

Abasic sites are known to significantly destabilize deoxyribooligonucleotide duplexes and to induce changes in duplex conformation in the vicinity of the site of base loss (*6*, *9*−*11*, *13*). A recent finding showed that when A bases were the flanking neighbors the duplexes were less destabilized, as characterized by the ΔT_m and $\Delta\Delta G^\circ_{37}$ values, than when C bases flanked the AP site (*14*). To determine whether this observation is a general phenomenon of the purine versus pyrimidine neighbors, 16 AP site-containing 15-mer duplexes were synthesized which contained all four possible symmetric double neighbors at the AP site and all four possible bases opposite the AP site in all combinations. Additionally, to calculate the differential destabilization values, the 16 corresponding control duplexes were also prepared. Thermodynamic parameters for the thermally induced strand dissociation for all duplexes were calculated from equilibrium absorption−melting temperature profiles (Tables 1−5).

All 15-mer duplexes were strongly destabilized by the single, site-specifically incorporated tetrahydrofuranyl AP site. The most important conclusion drawn from the analysis of thermodynamic data is that the less destabilized duplexes were those in which purine bases flanked the AP site. This was shown by both the ΔT_m and $\Delta\Delta G^\circ_{37}$ values when the opposite base was T, A, or C. In other words, flipping of the neighbor base pairs affects the extent of destabilization by an AP site. Thus, for 12 of the 16 duplexes, the average stabilizing effect of the symmetric doublet purine neighbors of an AP site was 3.2 °C for ΔT_m and 1.3 kcal/mol for $\Delta\Delta G^\circ_{37}$, as compared to the pyrimidine neighbors. When G is opposite the AP site, the neighbor-induced differential destabilization was also found to be smaller when the neighbor bases were AA or TT nucleotides. However, this effect was absent when CC or GG nucleotides were the flanking bases. Thus, 14 of 16 possible combinations of flanking sequences and opposite bases in the 15-mer AP duplexes yielded similar results.

The observation of the role of flanking bases is similar to our earlier finding with 15-mer AP duplexes (*14*). In that case, by replacement of C with A bases in the neighbor triplets, the difference between the ΔT_m values was 4−7 °C and decreased with increasing GC content. In the work presented here, these differences ranged from 1 to 8 °C, and with higher GC content, there was also less destabilization of the duplex by an AP site. The differences between $\Delta\Delta G^\circ_{37}$ values did not depend on the GC content. The duplexes with symmetric A neighbors were then less destabilized by about 1 kcal/mol than those with C neighbors (*1*). This difference is very similar to the average value calculated in our work (1.3 kcal/mol). The importance of the sequence context with respect to the thermodynamic consequences of the formation of an abasic site was recently reported by Gelfand et al. (*6*). Their data showed that duplexes containing the GxG motif were less destabilized than the duplexes with the CxC motif, thus supporting the idea of a differential effect of the purine versus pyrimidine neighbors on the AP site-induced destabilization.

The differences in the relative stabilizing effect caused by purine neighbors, as compared to pyrimidine neighbors, can be found in the differential enthalpy destabilization. The enthalpy value (ΔH°), which is thought to be influenced by base stacking, was always smaller, by about 20 kcal/mol, when pyrimidine bases flanked the AP site than when purine bases were the immediate neighbors. A connection to the enthalpy is more pronounced when the changes in the ΔH° values of the AP duplexes, compared to the ΔH° values of the control duplexes, are compared, that is, when the differential enthalpy values ($\Delta\Delta H^\circ$) are calculated and used.

Duplexes with purine neighbors at the AP site had smaller $\Delta\Delta H^\circ$ values than those with pyrimidines. The average $\Delta\Delta H^\circ$ was −42.3 and −25.7 kcal/mol for duplexes with flanking TT (duplexes 17, 21, 25, and 29) and AA bases (duplexes 18, 22, 26, and 30), respectively. The average $\Delta\Delta H^\circ$ was −32.4 and −21.5 kcal/mol for duplexes with CC (duplexes 19, 23, and 27) and GG flankings (duplexes 20,

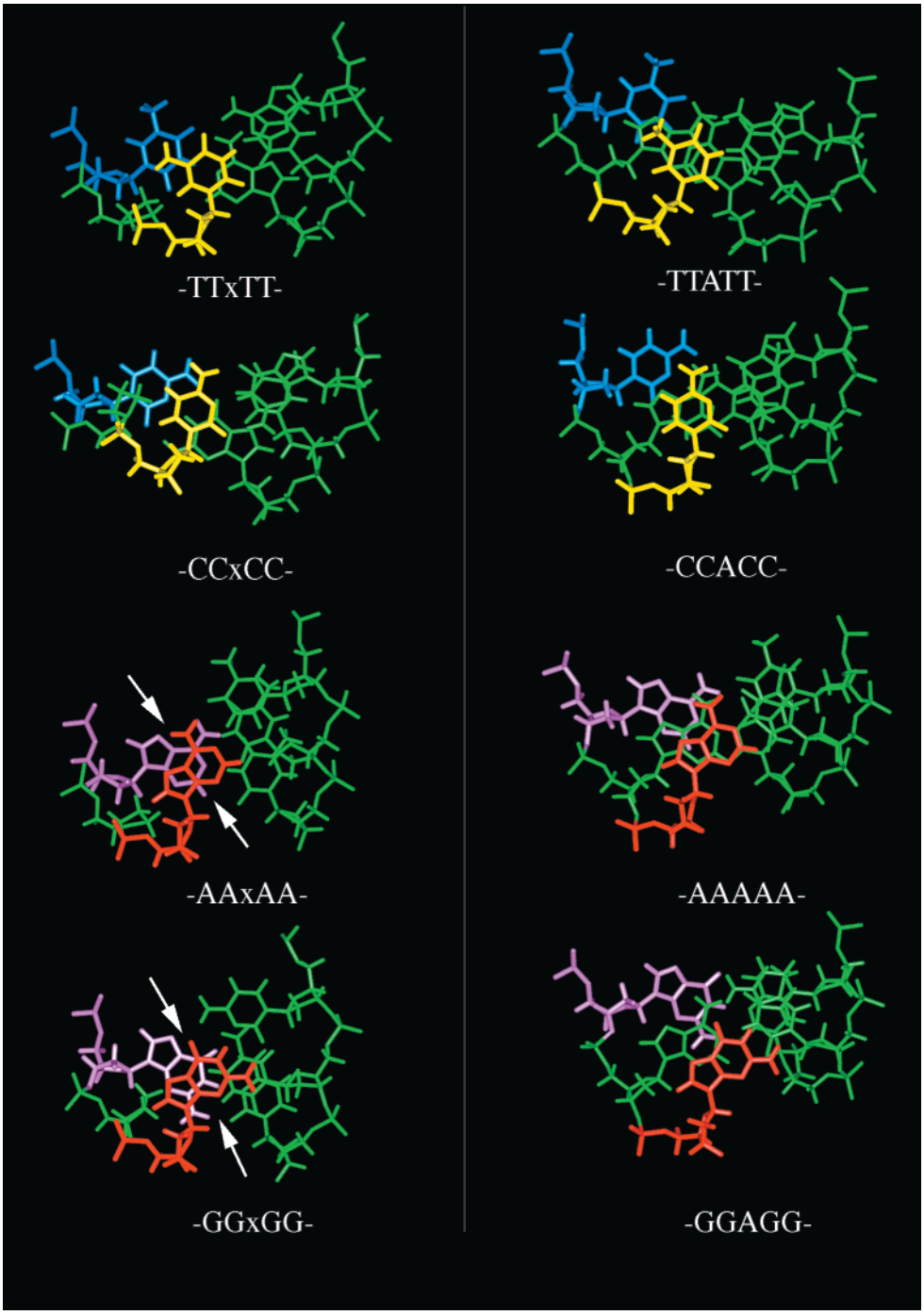

FIGURE 2: Top view of the central 3 bp motif of all eight averaged minimized structures produced by molecular dynamics simulations. The left panel shows the AP-containing structures, and the right panel shows the corresponding controls (AP is x). To visualize the overlap between the bases flanking the lesion site (or the central A base in controls), the pyrimidines flanking the AP site, or the central A base in controls, are shown in blue at the 5′ end and yellow at the 3′ end. The purines at the 5′ end are shown in light purple and at the 3′ end in red. Note the significant overlap between the purines flanking the AP site in the AAxAA and GGxGG structures (indicated by arrows).

24, and 28), respectively. The smaller $\Delta\Delta H°$ values are likely to indicate better stacking interactions at the AP site.

For duplexes with an AP·G pair and TT or AA neighbors, the $\Delta\Delta H°$ values were almost as high as those for the duplexes with T, A, or C opposite bases. However, the differential effect on enthalpy by the neighbors almost disappeared in the $\Delta\Delta G°_{37}$ values (only 0.12 kcal/mol vs the average value of 1.3 kcal/mol). For the AP·G duplexes with CC or GG neighbors, only very small $\Delta\Delta H°$ values were observed: −11.3 kcal/mol for duplex 31 and −6.5 kcal/mol for duplex 32. Thus, unpaired G diminished the negative effect of a base loss on enthalpy and also the differential effect of the neighbor bases, although the global stability for the duplexes with the CCxCC-/G and GGxGG-/G central sequences also decreased significantly, as reflected by the $\Delta\Delta G°_{37}$ values. These decreases were among the smallest that were observed. The G opposite T (T·G mismatch) and other exocyclic base adducts were also recently shown to cause the smallest duplex destabilization (*25*).

Our calculations for the duplexes with a T, A, or C base opposite the AP site can be interpreted as showing that the purine neighbors, due to their potentially higher base−base

overlapping energy, tend to close the gap created by the loss of a base more than pyrimidine neighbors (*20*). Molecular dynamics simulations were carried out with a selected group of structures (four structures containing T opposite the AP site and corresponding controls; Scheme 1, where M is T and x is an AP site or adenine) to prove or reject the conclusion of the thermodynamic calculations.

Previously, it had been shown that the presence of mismatch sites can alter DNA flexibility and curvature and thus affect DNA−protein interactions, including recognition (*23*, *37*−*40*). Recent modeling and NMR studies demonstrated that the presence of the AP site alters the DNA curvature (*12*, *21*, *22*). Our values for DNA curvature in the structures with the pyrimidines flanking the AP site (TTxTT and CCxCC) were larger than those for the structures with the purine bases flanking the AP site (AAxAA and GGxGG) (Table 7). A similar observation can be made for some of the curvature data reported by Ayadi et al. (*21*, *22*). This group measured a larger curvature for the 11-mer DNA structure with the TCxCT/AGTGA central duplex (26°) than for the DNA duplex containing the TGxGT/ACTCA central motif (15°). The smaller values observed by us for the CCxCC and GGxGG structures (19° and 12°, respectively) can be associated with the presence of two extra GC base pairs at the AP site, which should reduce the DNA flexibility. The difference in curvature between the TTxTT or CCxCC and AAxAA or GGxGG structures can be related to the observed different degree of overlap between the neighboring AP site bases. The tendency to stack two T or C bases flanking the AP site is weaker than for the A or G bases. This might result in the large kink at the central sequence for the TTxTT and CCxCC duplexes. The pronounced kink correlates with the observed larger values of roll for the unpaired T and reduced twist value for the preceding base pair (Table 6). We cannot state that the increase in DNA curvature for the central base pairs in the structures with the pyrimidines flanking the AP site primarily depends on the weaker stacking interaction between these bases. The magnitude of the DNA curvature can result from a large number of small perturbations in the DNA duplex, including the roll and/or tilt parameters.

The differential curvatures observed for duplexes with purine or pyrimidine neighbors could be an indication that the local conformation at the bending site, at or near the AP site, depends on the neighbors. The top views of the central three base pairs of all eight duplexes used in simulations were selected and are shown in Figure 2. It clearly shows that when purine bases are flanking the AP site, they tend to move toward positions that seem to be overlapping from this top view. The distant overlapping may provide stacking energy, which compensates for part of the destabilization caused by the loss of a base. Similar overlapping was not observed when pyrimidines were flanking the AP site. We should point out that in all four structures produced by molecular dynamics the opposite T remained stacked into the helix. This can be influenced by the fact that the intrahelical position of the opposite T was modeled in the starting structures, assuming that this conformation is more stable than extrahelical. Moreover, the length of the simulations (500 ps) could be considered rather short for adequately sampling both intra- and extrahelical conformations for the unpaired base. The MD of larger length using different starting structures containing both extra- and intrahelical positions of the base opposite AP site can be used in the future to validate our observations. It is reasonable to assume that in some DNA duplexes used for thermodynamics measurements the opposite base might be in an extrahelical position. However, we expect that the tendency of the two purines flanking the AP site to stack still will be higher than that of the two pyrimidines, thus compensating partially for the thermodynamically observed destabilization.

The differences in the local conformation at the AP site may provide an explanation for the observed differential thermodynamic destabilization by an AP site, which is dependent on whether purine or pyrimidine bases are flanking the AP site opposite a T, A, or C base.

REFERENCES

1. Loeb, L., and Preston, B. (1986) *Annu. Rev. Genet. 20*, 201−230.
2. Lindahl, T., and Nyberg, B. (1972) *Biochemistry 11*, 3610−3618.
3. Demple, B., Harrison, L., Wilson, D. M., Bennett, R. A. O., Takagi, T., and Ascione, A. G. (1997) *Environ. Health Perspect. 105*, 931−934.
4. Doetsch, P. W. (1995) *Trends Biochem. Sci. 20*, 384−386.
5. Barzilay, G., Walker, L. J., Robson, C. N., and Hickson, I. D. (1995) *Nucleic Acids Res. 23*, 1544−1550.
6. Gelfand, C. A., Plum, G. E., Grollman, A. P., Johnson, F., and Breslauer, K. J. (1998) *Biochemistry 37*, 7321−7327.
7. Shida, T., Arakawa, M., and Sekiguchi, J. (1994) *Nucleosides Nucleotides 13*, 1319−1326.
8. Ide, H., Shimizu, H., Kimura, Y., Sakamoto, S., Makino, K., Glackin, M., Wallace, S. S., Nakamuta, H., Sasaki, M., and Sugimoto, N. (1995) *Biochemistry 34*, 6947−6955.
9. Goljer, I., Withka, J. M., Kao, J. Y., and Bolton, P. H. (1992) *Biochemistry 31*, 11614−11619.
10. Goljer, I., Kumar, S., and Bolton, P. H. (1995) *J. Biol. Chem. 270*, 22980−22987.
11. Withka, J. M., Wilde, J. A., Bolton, P. H., Mazumder, A., and Gerlt, J. A. (1991) *Biochemistry 30*, 9931−9940.
12. Wang, K. Y., Parker, S. A., Goljer, I., and Bolton, P. H. (1997) *Biochemistry 36*, 11629−11639.
13. Beger, R. D., and Bolton, P. H. (1998) *J. Biol. Chem. 273*, 15565−15573.
14. Sagi, J., Hang, B., and Singer, B. (1999) *Chem. Res. Toxicol. 12*, 917−923.
15. Kalnik, M. W., Chang, C. N., Grollman, A. P., and Patel, D. J. (1988) *Biochemistry 27*, 924−931.
16. Cuniasse, P., Sowers, L. C., Eritja, R., Kaplan, B., Goodman, M. F., Cognet, J. A., Le Bret, M., Guschlbauer, W., and Fazakerley, G. V. (1989) *Biochemistry 28*, 2018−2026.
17. Kalnik, M. W., Chang, C. N., Johnson, F., Grollman, A. P., and Patel, D. J. (1989) *Biochemistry 28*, 3373−3383.
18. Barsky, D., Folloppe, N., Ahmadia, S., Wilson, D. M., III, and MacKerell, A. D., Jr. (2000) *Nucleic Acids Res. 28*, 2613−2626.
19. Cuniasse, P., Fazakerley, G. V., Guschlbauer, W., Kaplan, B. E., and Sowers, L. C. (1990) *J. Mol. Biol. 213*, 303−314.
20. Coppel, Y., Berthet, N., Coulombeau, C., Garcia, J., and Lhomme, J. (1997) *Biochemistry 36*, 4817−4830.
21. Ayadi, L., Coulombeau, C., and Lavery, R. (2000) *J. Biomol. Struct. Dyn. 17*, 645−653.
22. Ayadi, L., Coulombeau, C., and Lavery, R. (1999) *Biophys. J. 77*, 3218−3226.
23. Marathias, V. M., Jerkovic, B., and Bolton, P. H. (1999) *Nucleic Acids Res. 27*, 1854−1858.
24. Guliaev, A. B., Sagi, J., and Singer, B. (2000) *Carcinogenesis 21*, 1727−1736.
25. Sagi, J., Perry, A., Hang, B., and Singer, B. (2000) *Chem. Res. Toxicol. 13*, 839−845.

26. McDowell, J. A., and Turner, D. H. (1996) *Biochemistry 35*, 14077−14089.
27. Case, D. A., Pearlman, D. A., Caldwell, J. W., Cheatham, T. E., Ross, W. S., Simmerling, C. L., Darden, T. A., Merz, K. M., Stanton, R. V., Cheng, A. L., Vincent, J. J., Crowley, M., Ferguson, D. M., Radmer, R. J., Seibel, G. L., Singh, U. C., Weiner, P. K., and Kolman, P. A. (1997) *Amber 5.0*, University of California, San Francisco.
28. Cornell, W. D., Kollman, P. A., and Ferguson, D. M. (1995) *J. Am. Chem. Soc. 117*, 5179−5191.
29. Miaskiewicz, K., Miller, J., Cooney, M., and Osman, R. (1996) *J. Am. Chem. Soc. 118*, 9156−9163.
30. Lavery, R., and Sklenar, H. (1996) *CURVES 5.1. Helical analysis of irregular nucleic acids*, Laboratory for Theoretical Biochemistry, CNRS, Paris.
31. Hang, B., Sagi, J., and Singer, B. (1998) *J. Biol. Chem. 273*, 33406−33413.
32. Pilch, D. S., Dunham, S. U., Jamieson, E. R., Lippard, S. J., and Breslauer, K. J. (2000) *J. Mol. Biol. 296*, 803−812.
33. Xia, T. B., SantaLucia, J., Burkard, M. E., Kierzek, R., Schroeder, S. J., Jiao, X. Q., Cox, C., and Turner, D. H. (1998) *Biochemistry 37*, 14719−14735.
34. SantaLucia, J., Allawi, H. T., and Seneviratne, A. (1996) *Biochemistry 35*, 3555−3562.
35. Jourdan, M., Garcia, J., Defrancq, E., Kotera, M., and Lhomme, J. (1999) *Biochemistry 38*, 3985−3995.
36. Neidle, S. (1999) *Oxford handbook of nucleic acid structure*, Oxford University Press, New York.
37. Marathias, V. M., Jerkovic, B., Arthanari, H., and Bolton, P. H. (2000) *Biochemistry 39*, 153−160.
38. Grove, A., Galeone, A., Mayol, L., and Geiduschek, E. P. (1996) *J. Mol. Biol. 260*, 196−206.
39. Grove, A., Galeone, A., Mayol, L., and Geiduschek, E. P. (1996) *J. Mol. Biol. 260*, 120−125.
40. Wang, Y. H., Bortner, C. D., and Griffith, J. (1993) *J. Biol. Chem. 268*, 17571−17577.

BI0024409